Rock physical properties controlling *P*-wave dispersion and attenuation in outcrop carbonate specimens

Lucas C. Oliveira[1], Roseane M. Missagia[1,2], Irineu de A. Lima Neto[1] and Marco A. R. de Ceia[1,2].
Petroleum Engineering and Exploration Laboratory (LENEP) – North Fluminense State University (UENF);
Instituto Nacional de Ciência e Tecnologia (INCT – GP)

This paper was prepared for presentation during the 15th International Congress of the Brazilian Geophysical Society held in Rio de Janeiro, Brazil, 31 July to 3 August, 2017.

Abstract

Seismic waves propagation in dry and saturated elastic media gives insight into the rock physical properties. The poroelasticity Biot theory provides us with a theoretical basis for understanding the phenomena of low-frequency seismic waves dispersion and attenuation due to wave-induced fluid flow. One of the most accepted mechanisms to explain the phenomenon of wave attenuation in saturated porous media is the fluid flow induced by the wave on the mesoscopic scale, i.e., a scale larger than the pore size and much smaller than the wavelength. This work has the aim of investigating the influence of petrophysical and elastic properties of rock parameters in P-wave dispersion and attenuation in carbonate samples. It was performed through laboratory evaluation, using static and dynamic measures of the P-wave velocity under dry and saturated conditions. Therefore, here we applied Gassmann and Geertsma and Smith (1961) approaches, for estimate P-wave dispersion, Dvorkin and Mavko (2006) model to estimate the attenuation and determination of the characteristic frequency by interlayer flow White *et al.* (1975) model on the mesoscopic scale.

Introduction

The study of rocks physical properties is important for reservoir characterization and monitoring. The compressional and shear velocities of rocks are strongly influenced by the frequency and exhibit velocity dispersion. Velocity dispersion originates different values for several measurement bandwidths frequencies as seismic reflection (< 200 Hz), acoustic logging (approximately 10^4 Hz), and laboratory ultrasonic (10^5 - 10^6 Hz), hindering the comparison and application of these velocities (Tao *et al.*, 2010).

Seismic waves lose energy during their propagation in an elastic medium and the amplitude decreases in function of distance from its source emitting (Schön, 2011). In an elastic medium, the seismic waves induce fluid pressure in porous space that results in an induced fluid flow, which may cause internal friction against the rock matrix. The viscous-flow friction transfers part of the energy into heat, resulting in attenuation of seismic wave (Tisato and Quintal, 2013; Dvorkin and Mavko, 2006).

This work aims to study the effect of *P*-waves dispersion and attenuation (*1/Q*) in carbonate rocks, through laboratorial evaluation from petrophysical, mechanical and acoustic data; application Gassmann (1951), Dvorkin and Mavko (2006) and Characteristic frequency models by White *et al.* (1975), using stress-train static and dynamic velocities measures in undrained condition and saturated with fluids simulation.

Data Set

The Edwards Plateau is one of the largest continuous karst regions in the USA, locating in the southernmost part of the Great Plains Physiographic Province, where relatively undeformed Cretaceous carbonate and clastic rocks deeply bury a thick sequence of fractured and intensely folded Paleozoic metasediments. The Edwards Limestone is the primary cavernous unit; its aquifer extends throughout the region as the major public water supply. This area possesses numerous geologic formations, as a result of persistent marine inundation, sedimentation, reef formation, and faulting events (Veni, 1994).The limestone throughout the region has undergone extensive erosion, resulting in the exposure of older limestone formations in some areas of the Edwards Plateau (*Figure 1*), while, in other areas, the Edwards limestone is still subsurface (Cooke *et al.*, 2007).

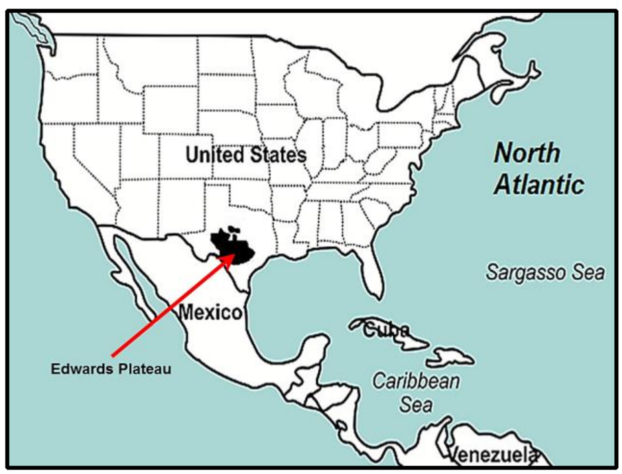

***Figure 1 –** Location map of Edwards Plateau in Texas, USA. Adapted from Oliveira et al (2016).*

This study uses four (4) limestone outcrop samples from Edwards Plateau, Texas, EUA. In the available samples the porosity ranges between 11.45-26.83% and permeability between 2.75-108.019 mD, as seen in *Tab 1.*

***Table 1 –** Mineralogical and petrophysical data (modified from Oliveira et al., 2014).*

Sample	ϕ (Gas)	k (mD)	a	K_m (GPa)	G_m (GPa)	ρ_{mr} (g/cm^3)
AC-01	0.2611	13.411	2.42	70.57	30.27	2.0024
DP-01	0.2683	118.019	2.37	70.68	30.36	1.9836
EW-02	0.1145	2.750	4.90	70.70	30.35	2.4032
EY-02	0.2365	47.534	2.62	70.79	30.36	2.0715

Theory

Velocity dispersion and frequency dependent

The Gassmann (1951) theory is widely used for fluid substitution. Gassmann equation gives a relationship between saturated bulk modulus (K_{sat}), porosity (ϕ), bulk modulus of rock in dry condition (K_{dry}), bulk modulus of mineral matrix rock (K_m) and the bulk modulus of pore fluids (K_{fl}):

$$K_{sat} = K_{dry} + \frac{\left(1 - \frac{K_{dry}}{K_m}\right)^2}{\frac{\phi}{K_{fl}} + \frac{1-\phi}{K_m} - \frac{K_{dry}}{{K_m}^2}}. \tag{1}$$

This equation indicates that fluid in pores will effect bulk modulus but not shear modulus, i.e. $\mu_{sat} = \mu_{dry}$. Gassmann equation estimates the seismic wave velocities in fluid-saturated porous media in low-frequency limit (<100Hz). Gassmann equation is much utilized by the petroleum industry for estimating seismic wave velocities in hydrocarbon reservoirs The compressional and shear velocities of rocks are strongly influenced by the frequency and exhibit velocity dispersion (Mavko *et al.*, 2009; Schön, 2011).

In order to study the frequency variation effect, Biot (1956) derived a theoretical formulation to estimate the frequency-dependent velocities of saturated rocks from dry-rock properties. This formulation proposed by Biot incorporates some mechanisms of viscoelastic interaction between the pore fluid and the mineral matrix of the rock (Mavko *et al.*, 2009). The incorporation of viscoelastic mechanisms results in: (1) velocity frequency dependence, i.e., velocity dispersion; (2) elastic wave attenuation in function of pore fluid viscosity. An important parameter between frequency and velocity relationships is the characteristic frequency (*fc*), this relation determines the low-frequency range (*f<<fc)* and high-frequency range (*f>>fc*) (Schön, 2011). For low-frequencies, the pore pressure excess induced by wave passage is dissipated, because the fluid accumulated in regions compressible move up to other pore space regions. Therefore, the fluid does not contribute to increasing of rock incompressibility. For high frequencies does not exist an equilibrium pressure because the fluid gets trapped in regions compressible of space pores, and the result this event is the velocity increase (Knight *et al.*, 1998).

Geertsma and Smith (1961) have proposed a formulation to get the velocities at high-frequency, $V_{p\infty}$ and $V_{s\infty}$, where:

$$V_{p\infty} = \sqrt{\frac{K_{dry} + \frac{4}{3}\mu_{dry} + \frac{\frac{\phi}{a}.\frac{\rho_{B\infty}}{\rho_{fl}} + \left(1 - \frac{K_{dry}}{K_m}\right)^2 . \left(1 - \frac{K_{dry}}{K_m} - 2.\frac{\phi}{a}\right)}{\left(1 - \frac{K_{dry}}{K_m} - \phi\right).\frac{1}{K_m} + \frac{\phi}{K_{fl}}}}{\rho_{B\infty}}}, \tag{2}$$

$$V_{s\infty} = \sqrt{\frac{\mu_{dry}}{\rho_{B\infty}}}, \tag{3}$$

$$\rho_{B\infty} = (1-\phi)\rho_m + \phi\rho_{fl}(1 - a^{-1}), \tag{4}$$

$\boldsymbol{\rho_{fl}}$ fluid density, ***a*** is the tortuosity parameter and $\boldsymbol{\rho_{B\infty}}$ is the bulk density at high-frequency. The velocities at low-frequency, $\boldsymbol{Vp_0}$ and $\boldsymbol{Vs_0}$, are obtained by:

$$V_{p0} = \sqrt{\frac{K_{sat_0} + \frac{4}{3}\mu_{dry}}{\rho_{B_0}}}, \tag{5}$$

$$V_{s0} = \sqrt{\frac{\mu_{dry_0}}{\rho_{B_0}}}, \tag{6}$$

$$\rho_{B_0} = (1-\phi)\rho_m + \phi\rho_{fl}. \tag{7}$$

The tortuosity can be obtained the following relationship

$$a = 1 - r.\left(1 - \frac{1}{\phi}\right), \tag{8}$$

where *r* = ½ for spheres, and between *0* and *1* for other ellipsoids. The high-frequency limiting velocities are strongly influenced by *a*, higher fast *P*-wave velocities have lower *a* values (Mavko et al, 2009).

For modeling elastic parameter and velocity frequency dependent, Geertsma and Smith (1961) derived an approximate solution for the Biot theory. Compressional wave velocity as a function of frequency (*f*) is:

$$V_p(f) = \sqrt{\frac{V_{p\infty}^4 + V_{p0}^4\left(\frac{f_c}{f}\right)^2}{V_{p\infty}^2 + V_{p0}^2\left(\frac{f_c}{f}\right)^2}}. \tag{9}$$

Dvorkin-Mavko attenuation model

Dvorkin and Mavko (2006) present a theory for calculate the P- wave inverse quality factor (*1/Q*) or attenuation at partial and full saturation. The basis for the quality factor estimation is the model that links the inverse quality factor (*1/Q*) to the corresponding elastic modulus *M* versus frequency (*f*) dispersion as

$$\frac{1}{Q(f)} = \frac{Im(M)}{Re(M)} \cong \frac{M_0 - M_\infty(f/f_c)}{\sqrt{M_0 M_\infty}[1 + (f/f_c)^2]}, \tag{10}$$

where M_0 and M_∞ are the low- and high-frequency limits of the modulus *M*, respectively; and *fc* is the critical frequency at which the inverse quality factor is maximum. The modulus *M* it is given by

$$M_{(0,\infty)} = K_{(0,\infty)} + {}^4/_3\,\mu_{(0,\infty)} = {V_{p(0,\infty)}}^2\rho. \tag{11}$$

Characteristic frequency models

When penetrating an elastic medium, the wave induces fluid pressure in porous space. For low-frequencies, not exist relative movement between the fluid and rock, because the fluid is trapped in the rock frame. For high-frequencies, the pressure gradient is responsible for the fluid flow, which when moving causes internal friction against the rock matrix, resulting in a relative movement between the fluid and rock frame. This fluid-flow type is known as the macroscopic fluid-flow (Biot, 1956; Tisato and Quintal, 2013). The dispersion mechanism is characterized by the f_c that establishes the frequency for which the attenuation and dispersion are maximum.

The primary cause of seismic attenuation in porous media at the low-frequency is presumably wave-induced fluid flow on the mesoscopic scale, i.e., the scale that is much larger than the pore size, but much smaller than the wavelength (White *et al.*, 1975; Toms *et al.*, 2006; Quintal *et al.*, 2009) Attenuation analytical models in mesoscopic scale have two major classifications, one considering the partial fluid saturation and other the lithological or mineral variation (Pride *et al.*, 2004).

White *et al.* (1975) were the first to introduce the mesoscopic loss mechanism providing a physically based model for low-frequency wave dispersion and attenuation. In the 1D interlayer-flow model, a partially saturated reservoir is represented by a laminated solid made of two periodically alternating layers of media 1 and 2 (White *et al.*, 1975; Norris, 1993; Carcione and Picotti, 2006). Each medium is a fully saturated poroelastic solid that differs by the pore fluid properties. Recent detailed descriptions of the interlayer-flow model can be showed in Carcione and Picotti (2006) and Quintal *et al.* (2009), and an approach for this model was given by Dutta and Seriff (1979) for a rock partially saturated with fluid. This approach is named interlayer-flow model characteristic frequency ($f_{C\text{-}IFM}$), separating the relaxed and unrelaxed states, given by

$$f_{C-IFM} = \frac{8kK_{E_1}}{\pi\eta_1 d_1^2}, \qquad (12)$$

were K_E is effective modulus of the saturated rock, *d* is the thickness of the saturated layer and the index *1* refers to the fluid-saturated layer.

Methodology

The relationship between frequency and elastic waves velocity can be studied indirectly by comparing data measured in a static and dynamic situation. The low-frequency (0 Hz) and high-frequency (10^6 Hz) velocities were obtained from elastic moduli in stress-strain static tests (low-frequency) and pulse transmission method (high-frequency) using a hydrostatic pressure (*HP*) system set up to work at 2.5 – 40.5 MPa effective pressure.

According to Tao *et al.* (2010), Gassmann velocity predictions obtained from dry velocity measurements can represent the zero-frequency velocity. Therefore, to analyze the partial fluid saturation effect in the dispersion and (*1/Q*) of *P*-wave in different frequencies, here we used the Gassmann model for estimate low-frequency velocities and Geertsma and Smith approach (*equation 2*) to estimate high-frequency velocities. The fluids properties used in this work are listed in *Table 2*.

Table 2 **–** *Fluids and mixture properties (Mavko et al., 2009[1]; Ball et al., 2002[2]; Toms et al., 2006[3]).*

	Fluid	K_f (GPa)	ρ_f (g/cm^3)	η (cPoise)
	Air[3]	0.0001	0.0012	0.0100
	Gas[3]	0.2500	0.4000	0.0600
	Oil[2]	0.7820	0.6970	0.3900
	Brine[1]	3.7977	1.0550	1.0000
Mixture	**Gas/brine**	0.4274	0.4328	0.1070
	Oil/brine	0.9328	0.7149	0.4205
	Brine/gas	3.6203	1.0223	0.9530

The central parameter of the *1/Q* and dispersion analyze of the velocity is the f_c, which separates a low-frequency and high-frequency ranges (Schön, 2011). In this work, f_c was obtained from interlayer-flow model (White *et al.*,1975), equation 12, which together with Vp_0, Vp_∞, M_0 and M_∞ allow applying Geertsma and Smith approach, equation 9, and Dvorkin-Mavko model, equation 10, for dispersion and *1/Q* velocity analyses.

Discussion and results

Quintal *et al.* (2009) considered interlayer flow caused by differences in the properties of the two-pore fluids aims to make an approach with partial water/gas saturation in which is also valid for other combinations of pore fluids, such as partial water/oil or oil/gas saturation. Therefore, in this study, we considered for heterogeneous saturation (summarized in *Table 2*): gas/brine (5% brine), oil/brine (5% brine) and brine/gas (5% gas). The laboratory experimental data necessary for development this work is summarized in *Table 3*.

The effect of dispersion and *1/Q* is observed from the ratio f_c/f (r_f). According to Gurevich (1996), at high-frequency (r_f <<1) the wave propagation causes a lower *1/Q*, contributing to energy balance of the waves motion in poroelastic media. In contrast, at low-frequencies (r_f>>1) the wave propagation is highly attenuating. Therefore, the dispersion and *1/Q* are maximum when f/fc=1 (Dvorkin and Mavko, 2006). *Figure 2a* and *b* display the correlation *P*-wave velocity *1/Q* and dispersion with increased *HP*. Viscosity and pressure impact the mobility of the fluid in the pore space. Wherefore, an increase in pressure and decrease in viscosity increases fluid mobility and decrease *1/Q*. Thus, velocity and *1/Q* show an opposite behavior in relation to the increase in pressure.

Figure 3 exhibits a correlation between P-wave velocity dispersion and *1/Q*, where it can be seen that increasing velocity wave dispersion induces an exponential growth of the *1/Q* according to the hydrostatic pressure applied to the medium.

In general, seismic waves velocity are influenced by the physical properties of rock and pressure applied, ie, more rigid rocks express higher velocities because of mainly these are characterized by a high bulk modulus (K), shear modulus (μ), young modulus (*E*) and low pore compressibility (C_{pp}), resulting in high values of P and S waves velocity (Oliveira *et al.*, 2014). Moreover, it increases the wave dispersion and *1/Q*. Static elastic moduli estimated in low pressure are lower than the dynamic ones, due to the presence of highly compliant cracks, which affects the static modulus differently. Furthermore, during static measurements, the rock is stressed at a slower rate than in dynamic measurements (Walsh and Brace, 1966; King, 1969; Cheng and Johnston, 1981).

Figure 4 displays four plots analyzing the hydrostatic pressure influence in low and high-frequency elastic moduli. The C_{PP} was calculated according to the methodology proposed by Oliveira *et al.* (2016). Observe that at low pressure, the difference between low and high-frequency elastic moduli increases. In contrast, at high pressure, this increment between elastic moduli is reduced. Correspondingly, the *EW-02* samples express (at high pressure) a higher *P*-wave velocity dispersion and *1/Q* to smaller C_{pp} values, lower ϕ and a higher difference between low and high-frequency elastic moduli. Inversely, the *AC-01* sample has higher C_{pp}, smaller difference between low and high-frequency elastic moduli, and shows less *P*-wave velocity dispersion and *1/Q.*

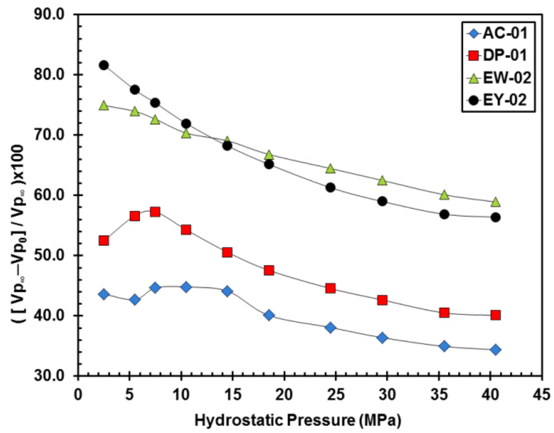

a)

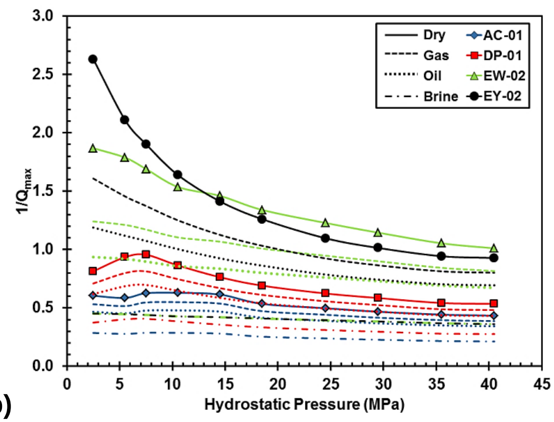

b)

Figure 2 *– Impact analyze of the Hydrostatic Pressure (HP) on (a) the P-wave velocity dispersion and (b) 1/Q under partial saturated and dry conditions. According to Dvorkin and Mavko model, 1/Q is maximum when f/fc=1.*

Table 3 *– Petrophysical, mechanical and acoustics data.*

Samples							
AC-01							
HP (MPa)	ϕ	ν_0	**E_0 (GPa)**	**Vp_0 (km/s)**	**Vp_∞ (km/s)**	**Vs_∞ (km/s)**	**C_{pp} (1/GPa)**
2.5	0.2606	0.270	6.09	1.951	3.461	2.047	0.245
5.5	0.2602	0.228	6.86	1.991	3.474	2.055	0.244
7.5	0.2599	0.179	6.84	1.925	3.477	2.056	0.243
10.5	0.2596	0.146	7.04	1.923	3.483	2.060	0.242
14.5	0.2593	0.111	7.41	1.950	3.490	2.061	0.241
18.5	0.2591	0.101	8.60	2.094	3.496	2.062	0.239
24.5	0.2588	0.083	9.26	2.165	3.496	2.062	0.239
29.5	0.2585	0.080	9.80	2.225	3.498	2.062	0.239
35.5	0.2582	0.065	10.31	2.276	3.500	2.062	0.238
45.5	0.2578	0.064	10.50	2.296	3.500	2.062	0.238
DP-01							
HP (MPa)	ϕ	ν_0	**E_0 (GPa)**	**Vp_0 (km/s)**	**Vp_∞ (km/s)**	**Vs_∞ (km/s)**	**C_{pp} (1/GPa)**
2.5	0.2680	0.132	6.32	1.822	3.834	2.249	0.184
5.5	0.2676	0.061	5.48	1.668	3.843	2.258	0.183
7.5	0.2673	0.047	5.35	1.645	3.847	2.261	0.183
10.5	0.2670	0.025	6.17	1.764	3.859	2.264	0.181
14.5	0.2668	0.020	7.23	1.909	3.861	2.265	0.181
18.5	0.2666	0.014	8.15	2.025	3.863	2.267	0.181
24.5	0.2663	0.015	9.15	2.145	3.869	2.267	0.180
29.5	0.2661	0.018	9.79	2.220	3.871	2.267	0.179
35.5	0.2658	0.013	10.55	2.303	3.871	2.267	0.179
40.5	0.2655	0.012	10.70	2.319	3.871	2.267	0.179
EW-02							
HP (MPa)	ϕ	ν_0	**E_0 (GPa)**	**Vp_0 (km/s)**	**Vp_∞ (km/s)**	**Vs_∞ (km/s)**	**C_{pp} (1/GPa)**
2.5	0.1137	0.050	3.41	1.194	4.765	2.434	0.123
5.5	0.1130	0.020	3.73	1.245	4.780	2.444	0.122
7.5	0.1127	0.019	4.11	1.308	4.780	2.451	0.123
10.5	0.1124	0.018	4.84	1.418	4.780	2.464	0.125
14.5	0.1120	0.013	5.28	1.481	4.783	2.468	0.125
18.5	0.1116	0.021	6.12	1.595	4.804	2.470	0.122
24.5	0.1113	0.019	7.02	1.708	4.804	2.472	0.123
29.5	0.1110	0.018	7.88	1.809	4.822	2.476	0.120
35.5	0.1107	0.016	8.93	1.925	4.826	2.478	0.120
45.5	0.1105	0.013	9.51	1.986	4.832	2.481	0.120
EY-02							
HP (MPa)	ϕ	ν_0	**E_0 (GPa)**	**Vp_0 (km/s)**	**Vp_∞ (km/s)**	**Vs_∞ (km/s)**	**C_{pp} (1/GPa)**
2.5	0.2361	0.023	1.19	0.758	4.131	2.159	0.129
5.5	0.2353	0.035	1.84	0.944	4.199	2.181	0.122
7.5	0.2351	0.017	2.24	1.041	4.218	2.192	0.120
10.5	0.2350	0.015	2.93	1.190	4.237	2.205	0.119
14.5	0.2348	0.011	3.76	1.347	4.237	2.208	0.119
18.5	0.2346	0.014	4.52	1.476	4.237	2.209	0.119
24.5	0.2344	0.016	5.59	1.642	4.241	2.209	0.119
29.5	0.2341	0.017	6.28	1.739	4.241	2.209	0.119
35.5	0.2338	0.012	6.95	1.829	4.241	2.209	0.119
45.5	0.2331	0.013	7.11	1.850	4.241	2.209	0.119

*Subscripts ***0*** and ∞ indicate low and high-frequency, respectively. ***E*** and ***ν*** are young modulus and poisson ratio, respectively, obtained in stress-strain static tests.

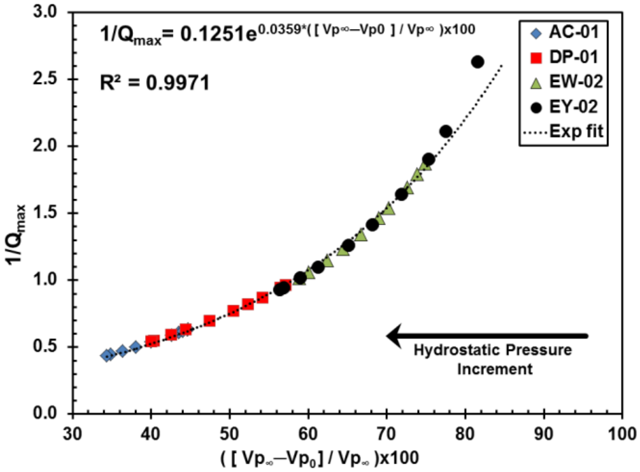

***Figure 3** – Comparison between P-wave velocity dispersion versus 1/Q in dry condition.*

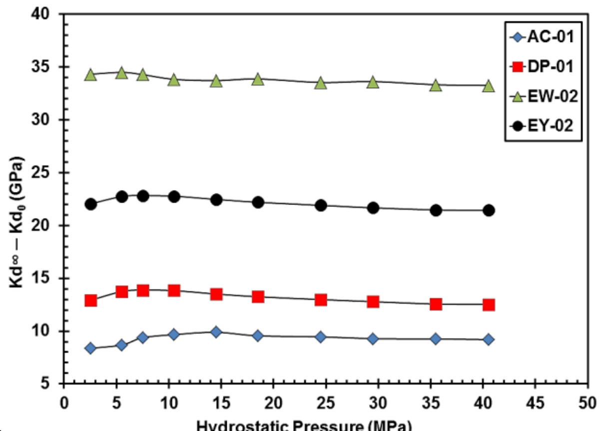

a)

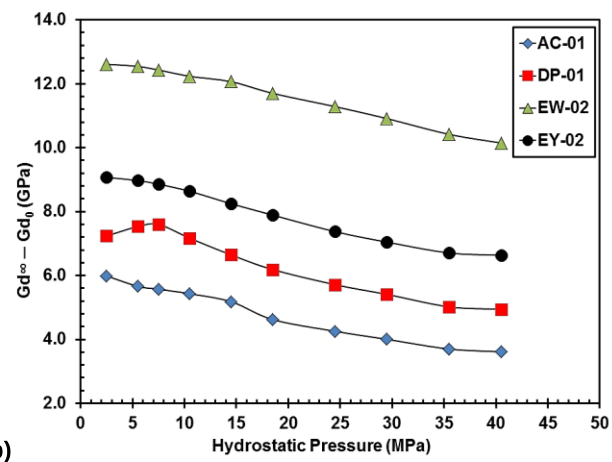

b)

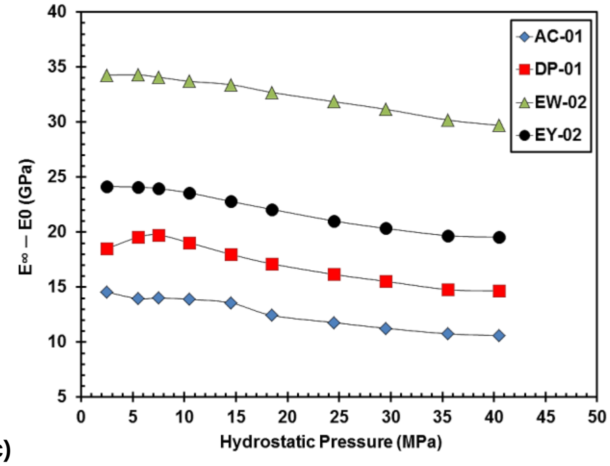

c)

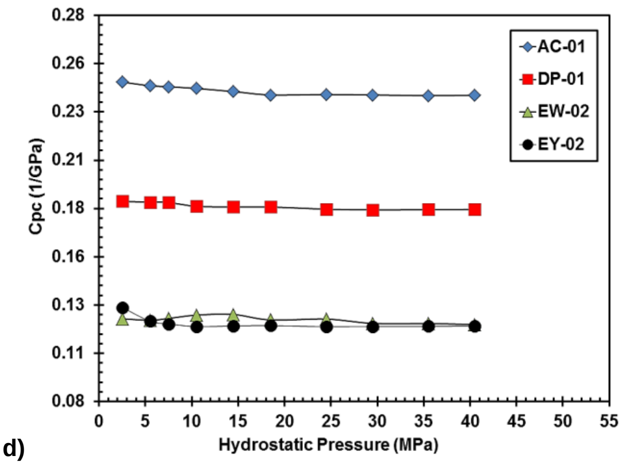

d)

***Figure 4** – High-frequency elastic moduli minus low-frequency elastic moduli (a-bulk modulus; b-shear modulus; c-young modulus) and (d) pore compressibility of carbonates core samples as a function of hydrostatic pressure. Elastic moduli are predicted from data on dry samples by stress-strain static test for low-frequency and by the ultrasonic velocities measurements for high-frequency.*

Conclusions

This work analyzed the P-wave propagation in the elastic medium under partial saturated and dry conditions. The petrophysical properties of the medium, such as porosity, permeability, fluid saturation and elastic properties of rock, are directly related to *P*-wave dispersion and attenuation. Results show that the correlation between velocity dispersion and 1/Q, elastic properties of rock can be a very useful tool for carbonates characterization.

Characteristic frequency calculated by the interlayer flow model on the mesoscopic scale proposed by White *et al.* (1975) is a good approximation for calculating the low-frequency and high-frequency limits.

The difference between the low and high-frequency moduli was shown to be much more significant at low pressures, because the elastic moduli estimated in low pressure are lower than the dynamic ones and more sensitive at pressure increment. Therefore, the samples with higher low and high-frequency elastic moduli difference and lower C_{pp} showed higher dispersion and attenuation. Furthermore, viscous effects cause decrease in 1/*Q* and dispersion of the P-wave velocity, higher fluid viscosity decreases *P*-wave dispersion and 1/Q.

Acknowledgments

We thank UENF/LENEP for facilities, and PRH-20 and PRH-226 to sponsor this study.

References

Ball, S. J., Goodwin, A. R. H., Trusler, J. P. M., 2002, Phase behavior and physical properties of petroleum reservoir fluids from acoustic measurements. Journal of Petroleum Science and Engineering, 34, 1-11.

Biot, M.A., 1956, Theory of propagation of elastic waves in a fluid saturated porous solid. I. Low frequency range and II. Higher-frequency range.J. Acoust. Soc. Am., 28, 168–191. http://dx.doi.org/10.1121/1.1908239

Carcione, J. M., and S. Picotti, 2006, P-wave seismic attenuation by slow-wave diffusion: Effects of inhomogeneous rock properties. Geophysics, 71(3), O1-O8. Doi: http://dx.doi.org/10.1190/1.219452

Oliveira, G. L. P., Ceia, M. A. R., Missagia, R. M., Archilha, N. L., Figueiredo, L., Santos, V. H., Lima Neto, I.,2016, Pore volume compressibilities of sandstones and carbonates from Helium porosimetry measurements. Journal of Petroleum Science and Engineering, 137, 185-201. Doi: http://dx.doi.org/10.1016/j.petrol.2015.11.0220920-4105/&2015

Cheng, C.H. and Johnston, D.H. 1981, Dynamic and static moduli. Geophys. Res. Lett., 8, 39-42. Doi: http://dx.doi.org/10.1029/GL008i001p00039

Cooke, M. J., Stern, L. A., Banner, J. L., Mack, L. E., 2007, Evidence for the silicate source of relict soils on the Edwards Plateau, central Texas. Quaternary Research, 67, 275–285. doi:10.1016/j.yqres.2006.11.007.

Dutta, N. C., and A. J. Seriff, 1979, On White's model of attenuation in rocks with partial gas saturation: Geophysics, 44, 1806–1812.

Dvorkin, J.P. and Mavko, G., 2006, Modeling attenuation in reservoir and non-reservoir rock. Leading Edge, 25, 194–197. Doi: http://dx.doi.org/10.1190/1.2172312

Gassmann, F., [1951] Uber die elastizitat poroser medien, Verteljahrss-christ der Naturforschenden Gesellschaft in Zurich, 96, 1 – 23.

Geertsma, J. and Smit, D.C., 1961, Some aspects of elastic wave propagation in fluid-saturated porous solids. Geophysics, 26(2), 169–181. Doi: http://dx.doi.org/10.1190/1.1438855

Gurevich B., 1996, Discussion on: Wave propagation in heterogeneous, porous media: A velocity stress, finite difference method, by N. Dai, A. Vafidis and E.R. Kanasewich (March April 1995 Geophysics, pp. 327–340), Geophysics, 61, 1230–1232.

King, M.S. 1969. Static and dynamic elastic moduli of rocks under pressure. 11th U.S. Symposium on Rock Mechanics. American Rock Mechanics Association. Berkeley. California.

Knight, R.; Dvorkin, J.; Nur, A., 1998, Acoustic Signatures of Partial Saturation, Geophysics, vol. 63 (1), p. 132-138. Doi: http://dx.doi.org/10.1190/1.1444305

Mavko, G., Mukerji, T. and Dvorkin, J. 2009, The Rock Physics Handbook, Tools for Seismic Analysis of Porous Media, 2nd edition. 511.

Norris, A. N., 1993, Low-frequency dispersion and attenuation in partially saturated rocks: Journal of Acoustical Society of America, 94, 359–370.

Oliveira, L.C., Lima Neto, I.A., Misságia, R.M., Ceia, M.A.R., Archilha, N.L., Castro, L.T, Souza, F.R., 2014, Elastic Properties Characterization and Pore System Evaluation Using Kuster-Toksöz and Gassmann Models, Amsterdam, 76th EAGE Conference & Exhibition. Doi: http://dx.doi.org/10.3997/2214-4609.20140873

Pride, S. R., Berryman, J. G., Harris, J. M., 2004, Seismic attenuation due to wave-induced flow. Journal of Geophysical Research, 109, B01201.

Quintal, B., Schmalholz, S. M., and Podladchikov, Y. Y., 2009, Low-frequency reflections from a thin layer with high attenuation caused by interlayer flow. Geophysics, 74(1), N15-N23. Doi: http://dx.doi.org/10.1190/1.3026620

Schön, J.H., 2011, Physical properties of rocks: Fundamentals and Principles of Petrophysics, Elsevier, Vol. 8.

Tao, H., Chang-Chun, Z., and Fa-Gen, P., 2010, Laboratory study of fluid viscosity induced ultrasonic velocity dispersion in reservoir sandstones. Applied Geophysics, 7(2), 114 – 126. Doi: http://dx.doi.org/10.1007/s11770-010-0235-3

Tisato, N., and Quintal, B., 2013, Measurements of seismic attenuation and transient fluid pressure in partially saturated Berea sandstone: evidence of fluid flow on the mesoscopic scale. Geophysical Journal International, 195, 342-531. http://dx.doi.org/10.1093/gji/ggt259

Toms, J., T. M. Mueller, R. Ciz, and B. Gurevich, 2006, Comparative review of theoretical models for elastic wave attenuation and dispersion in partially saturated rocks: Soil Dynamics and Earthquake Engineering, 26, 548–565

Veni, G. 1994, Hydrogeology and evolution of caves and karst in the southwestern Edwards Plateau, Texas. Pp. 13–30, in The Caves and Karst of Texas (W. R. Elliott and G. Veni, eds.). National Speleological Society, Huntsville, Alabama. 252 pp.

Walsh, J. and Brace, W. 1966, Elasticity of rock: a review of some recent theoretical studies. Rock Mechanics and Engineering Geology, 4. 283-297. International Society of Rock Mechanics. SpringerVerlag

White, J. E., N. G. Mikhaylova, and Lyakhovitskiy, F. M., 1975, Low-frequency seismic waves in fluid saturated layered rocks, Izvestija Academy of Sciences USSR, Physics of the Solid Earth,11, 654–659. Doi: http://dx.doi.org/10.1121/1.1995164